HOSTED BY

ELSEVIER

CrossMark

Available online at www.sciencedirect.com

ScienceDirect

Progress in Natural Science: Materials International 25 (2015) 185–190

Progress in Natural Science Materials International

www.elsevier.com/locate/pnsmi
www.sciencedirect.com

Original Research

The effect of swelling agent on the pore characteristics of mesoporous hydroxyapatite nanoparticles

L. Bakhtiari[a,*], J. Javadpour[a], H.R. Rezaie[a], M. Erfan[b], M.A. Shokrgozar[c]

[a]School of Metallurgical and Materials Engineering, Iran University of Science and Technology, Tehran, Narmak 16844, Iran
[b]School of Pharmacy, Shahid Beheshti University of Medical Sciences, Tehran 6153-14155, Iran
[c]National Cell Bank of Iran, Pasteur Institute of Iran, Tehran 13164, Iran

Received 14 October 2014; accepted 17 December 2014
Available online 15 July 2015

Abstract

The effect of swelling agent on the physicochemical properties of mesoporous hydroxyapatite particles synthesized by self-assembly process has been investigated. Cetyl trimethylammonium bromide (CTAB) and 1-dodecanethiol were used as soft template and swelling agent respectively. The results of the field emission scanning electron microscopy (FESEM), X-ray diffraction (XRD), simultaneous thermal analysis (STA), Brunauer-Emmett-Teller (BET) surface area, small-angle X-ray diffraction and Fourier transform infrared spectroscopy (FTIR) assessments revealed that in the case of low concentration, 1-dodecanethiol performed as swelling agent and caused an increase in the pore size. However, at higher concentrations it led to the formation of microemulsion and foamy structures. The optimum swelling agent: surfactant mass ratio in synthesis of mesoporous hydroxyapatite particles with high pore volume was determined to be around 2.1 in this study.

Keywords: Mesopore; Hydroxyapatite; Nanoparticle; Swelling agent; Pore characteristics

1. Introduction

Mesoporous materials possessing large surface areas and uniform pore size distributions have attracted much attention due to their potential applications in catalysis, gas sensing, adsorption, optics, polymer filler, bone tissue engineering, and drug delivery systems [1–4]. The synthesis of mesoporous materials is of considerable interest and is constantly being developed to explore new applications. Basically there are two major strategies for the synthesis of mesoporous materials, a soft templating method and a hard templating approach [5]. The soft templating mechanism makes use of the self-assembling ability of the surfactant molecules to produce a variety of well-organized porous inorganic materials. In the hard templating approach, a porous framework is used as a hard template. Mesostructure materials are obtained after the removal of the framework by combustion treatment or a chemical etching process. An important characteristic of the mesoporous materials is the possibility to control pore structural properties such as surface area, pore size, and pore volume. The latter parameters are critically important in the accommodation and release behavior of complex chemicals, catalytic reactions, and in controlled release of drugs [6]. One of the classical methods to adjust pore size is the use of organic swelling agent [7,8]. The basic principle is to change the size of the pore by changing the size and volume of the micelle structure. Swelling molecules usually move into the hydrophobic core of the micelle structure and expands them, thereby increasing the pore size of the materials. Inspired by this method, here we report the preparation of mesoporous hydroxyapatite (HAp) particles using 1-dodecanethiol as swelling agent. Synthesized hydroxyapatite (HAp) due its biocompatibility and ability to bond with living tissues has significant applications in the biomedical fields [9]. Moreover, the use of mesostructured HAp particles as delivery

*Corresponding author. Tel.: +98 21 77240480.
E-mail address: lbakhtiari@iust.ac.ir (L. Bakhtiari).
Peer review under responsibility of Chinese Materials Research Society.

http://dx.doi.org/10.1016/j.pnsc.2015.06.005

vehicle for a variety of pharmaceutical molecules has also been reported in the literature [9–22]. Synthesized materials with tunable pore size, pore volume and surface area are expected to further the application of these materials and allow for better control over the drug loading and release behavior. The effect of swelling agent on the pore characteristics in the synthesis of mesoporous HAp particles by soft templating method is reported in this study.

2. Materials and methods

Cetyl trimethylammonium bromide (CTAB), sodium hydroxide (NaOH), 1-dodecanethiol ($C_{12}SH$), calcium nitrate ($Ca(NO_3)_2 \cdot 4H_2O$), ortho phosphoric acid (85% purity) and ammonia solution (25% extra pure) were obtained from MERCK Company. CTAB and 1-dodecanethiol were used as dual templates. In a typical synthesis procedure, an emulsion containing 100 ml 30 mM CTAB in deionized water, 2.5 ml 1-dodecanethiol and 5 ml of NaOH solution (2 M) was prepared and stirred at 80 °C for 30 min. 10 ml of each hydroxyapatite precursors (0.01 M calcium nitrate, and 0.006 M ortho phosphoric acid) were added to the above solution and stirred for another 2 h. The pH of the final solution was adjusted by ammonia solution at 12. The resulting white precipitate was filtered, washed and dried at 60 °C overnight. The final dried powder was calcined at 550 °C for 5 h. The details of synthesized samples are summarized in Table 1. The crystallographic structure of synthesized samples was characterized by powder X-ray diffraction (XRD) using a Jeol, JDX-8030 Diffractometer. The degree of ordering in the pore structure was investigated using small angle X-ray diffraction (SAXRD; PANalytical, X'Pert PRO MPD). Fourier transform infrared (FTIR) spectra were collected on a Shimadzu, 8400s spectrometer. Simultaneous thermal analysis (STA; Netztch, PL STA 1640) was used to confirm the absence of surfactant in the synthesized powder. The morphology of the products was observed by field emission scanning electron microscopy (FESEM; Hitachi, S4160). The specific surface areas of the samples were calculated according to the Brunauer-Emmett-Teller (BET) method using adsorption data in the relative pressure P/P_0 range of 0.05–0.2. The pore size distributions were estimated using adsorption branch of nitrogen isotherms based on the Barrett, Joyner, and Halenda (BJH) model. The pore volumes were determined from the amount of N_2 adsorbed (Bellsorp mini-II) on the mesoporous samples.

Table 1
Summary of R values (CTAB: C_{12}–SH) mass ratios and their corresponding sample codes.

Sample code	R (C_{12}–SH/CTAB mass ratio)	1-dodecanethiol (C_{12}–SH) (ml)	CTAB (mM)
R2	2.11	2.5	30
R3	4.22	5	30
R4	6.33	7.5	30

3. Results and discussion

3.1. Phase identification

The XRD patterns for the calcined samples are presented in Fig. 1. The diffraction patterns for all three samples are in good agreement with the structural model of single phase hydroxyapatite (PDF file no.09-0432) in the ICDD data base [23]. Apparently, the change in the R values did not have a significant effect on the formation of HAp structure. The FTIR spectra of CTAB, 1-dodecanethiol, and calcined samples are displayed in Fig. 2. The absorption bands at –SH (3000–3200 cm^{-1}) and C–S (720–570 cm^{-1}) and the absorption band at CH_2– (3000 cm^{-1}) are characteristics bands for C_{12}–SH molecules and CTAB surfactant molecules respectively. The disappearance of these bands in the calcined samples is an indication that washing with deionized water and calcination at 550 °C for 5 h was sufficient for the removal of the swelling agent and surfactant molecules. FTIR spectra for the R2, R3 and R4 samples show characteristic bands of hydroxyapatite

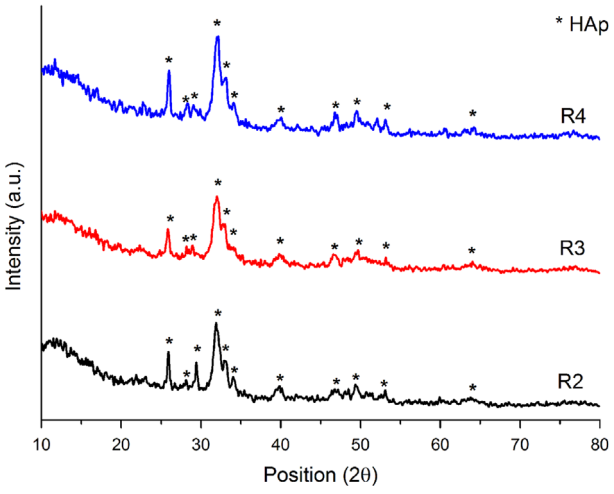

Fig. 1. XRD patterns of the samples calcined at 550 °C.

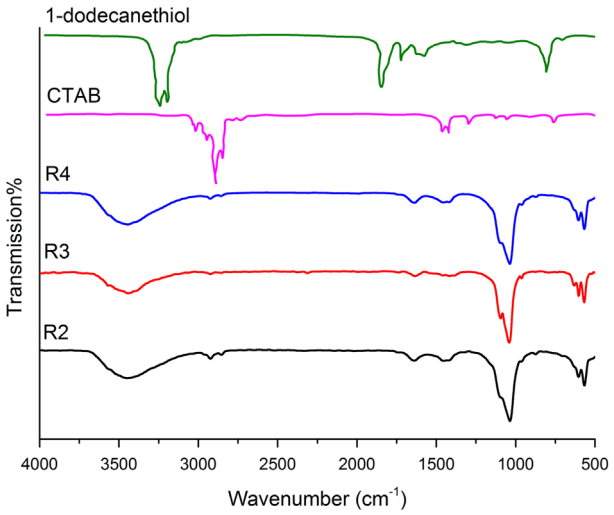

Fig. 2. FTIR spectra of the indicated samples.

structure (PO_4^{-3} group at 570 and 1047 cm^{-1}, CO_3^{-2} group at 1400–1500 cm^{-1} and hydroxyl at about 3300 cm^{-1}) confirming the XRD results. The thermal properties of the R4 sample containing the highest amount of swelling agent and surfactant molecules was studied by STA analysis (Fig. 3). The exothermic peak around 300 °C and the associated weight loss is related to the combustion and removal of surfactant molecule [17]. As indicated in this profile, the process of weight loss was stabilized at about 500 °C. The choice of calcination temperature in this study (550 °C) was based on the STA results.

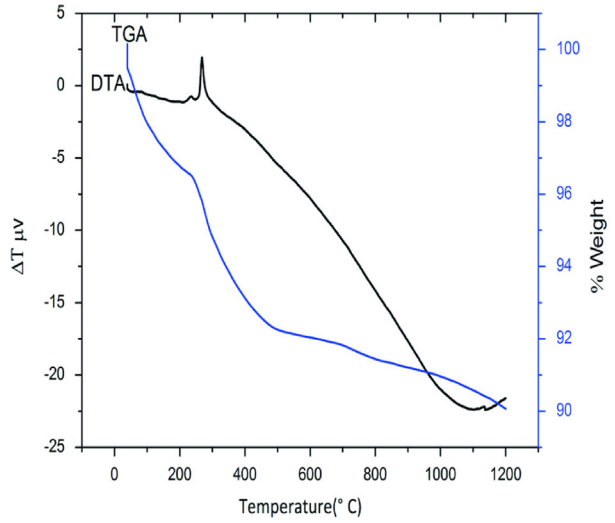

Fig. 3. STA profile of the as-prepared R4 sample.

3.2. Morphology and pore characteristics

The main objective in the present study is to study the effect of swelling agent concentration on the properties of mesoporous hydroxyapatite particles. The results of previous studies on micellar structure in the absence of swelling agent, shows the formation of spherical micelles at low CTAB:PO_4^{-3} molar ratio (about 0.06) [18], and the formation of cylindrical (rod-like) hydroxyapatite particles at higher CTAB:PO_4^{-3} ratios [17,24,25]. The formation of cylindrical particles in the absence of 1-dodecanethiol was observed in this study as well (FESEM image of R0 sample shown in Fig. 4). The results in the present investigation indicate that changes in the concentration of swelling agent leads to the formation of different micelle structures and consequently different pore morphologies (compare FESEM images of samples R2–R4 in Fig. 4). The initial addition of swelling agent causes the formation of rod shaped particles with larger diameters (compare FESEM images for samples R2 and R0). Close examination of Fig. 4 shows sphere like particles with approximate size of 50 nm for R3 sample and a foamy morphology for R4 sample. The effect of swelling agent on the morphology of the mesoporous structures has already been shown in the literature [26]. Apparently, the change in the degree of interaction between the tail groups of CTAB, the solvent and the swelling agent leads to the formation of different micelle structures and consequently different pore morphologies. As shown schematically in Fig. 5, cylindrical micelles formed at low concentration of swelling agent (sample R2). With the increase in the concentration, the hydrophobic C_{12}–SH molecules diffuse into the hydrophobic section of micelles (CTAB tail) and initiated the swelling process. Gradually the walls of the cylinders

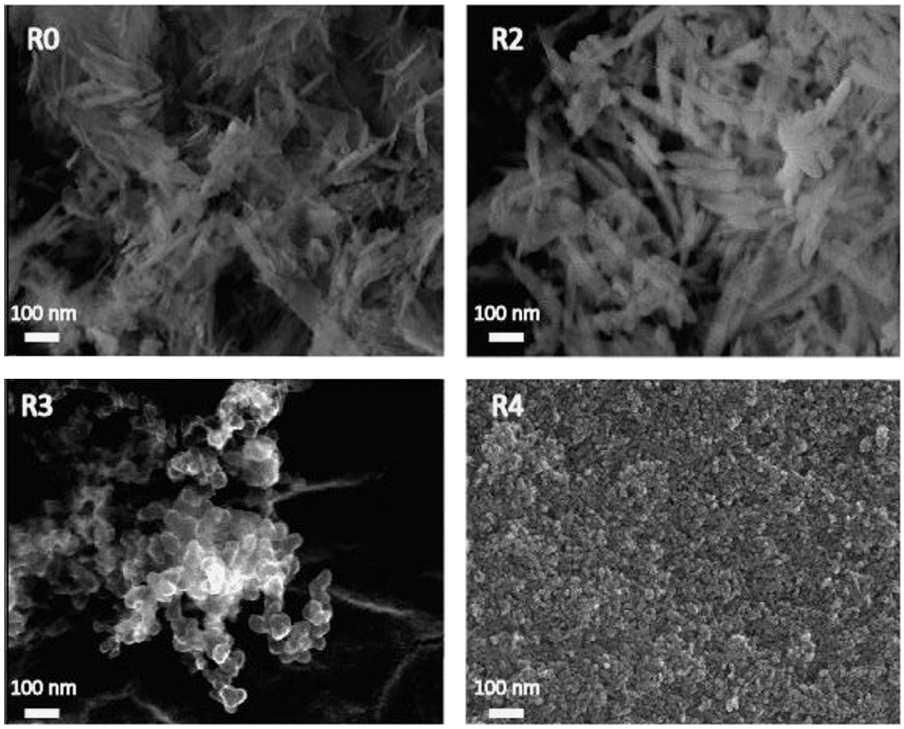

Fig. 4. FESEM micrographs of synthesized R0 sample in absence of swelling agent and R2–R4 samples in presence of swelling agent.

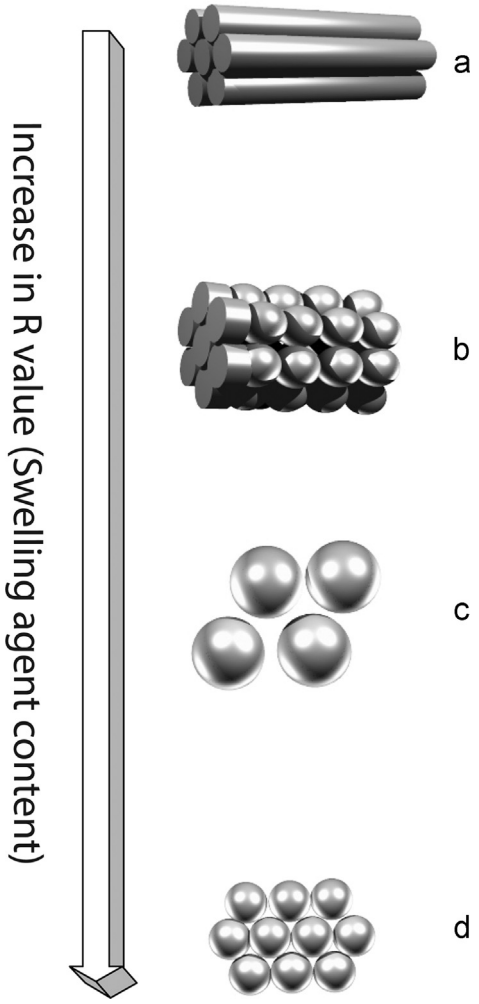

Fig. 5. Morphological changes in the micelle structure with the increase in R values (swelling agent content): rod-like micelles at low concentration of swelling agent (a), a transition to sphere shape with the increase in the swelling agent content (b), formation of sphere micelles (c) and formation of foamy structure (d).

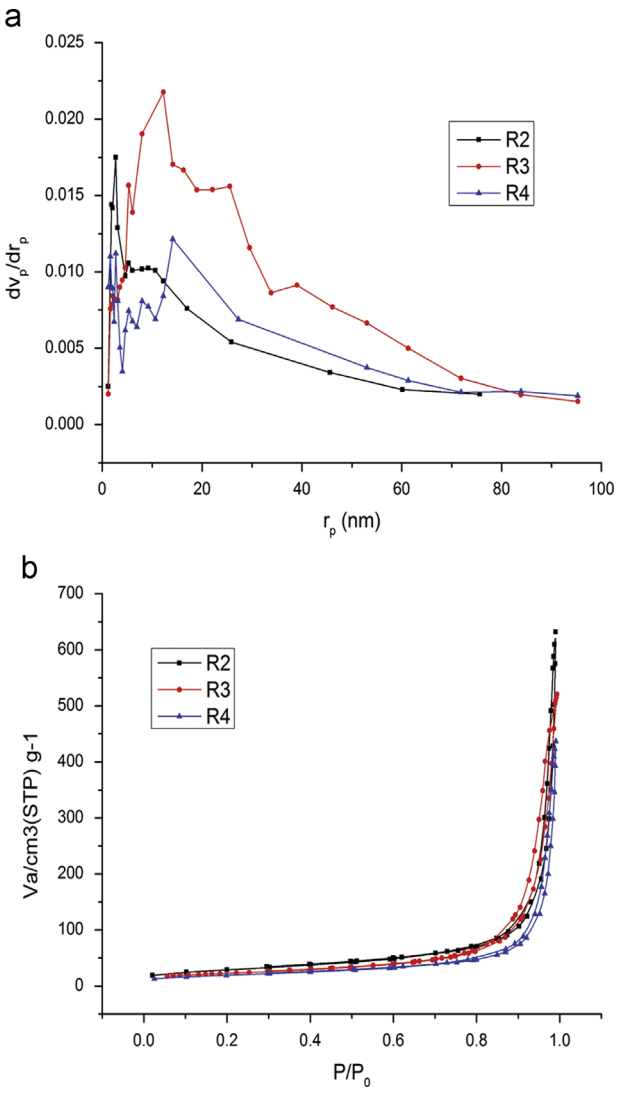

Fig. 6. Pore size distribution (BJH plots) for samples with different swelling agent content (a) and Nitrogen adsorption–desorption isotherms for the indicated samples (b).

began to buckle and nodes started to appear on the walls. These nodes can eventually break the cylinder micelle into spheres (sample R3). Further increase in swelling agent leads to the formation of foamy structure (sample R4). These changes are based on the packing factor parameter of surfactant ($g = v/al$) proposed by Israelachvili and co-workers [27]. In this equation, v is the effective volume of surfactant tail, a refers to the effective head group area and l is the length of surfactant tail. The increase in the swelling agent concentration lowers the surfactant packing factor (g) by the increase the effective head group area (a value). This in turn increases the CMC (Critical Micelle Concentration) as well as the N_{agg} (aggregation number) of the micelle resulting in an increased repulsive force, a decrease in micelle radius of curvature and a transition from particles with rod shape to particles with sphere shape [28,29]. Further increase in swelling agent concentration gives rise to foamy structure which is in good agreement with previously reported data in the literature [26,27]. Fig. 5 displays schematically the changes in the micelle structures (rod → sphere → foam) with the increase in the swelling agent content. Pore characteristic of the samples were studied by collecting nitrogen adsorption–desorption isotherms. Fig. 6(a) shows the pore size distributions determined by Barrettt, Joyner, and Halenda (BJH) method and part (b) shows the collected isotherm data for the samples R2–R4. Nitrogen adsorption–desorption isotherms for all the samples are of type IV according to IUPAC classification, indicating the formation of mesopores on all samples. The surface area, pore volume and the average pore diameter size for the calcined samples are summarized in Table 2. As indicated in this table, with the increase in the R values (increase in swelling agent), there is a decrease in surface area, pore volume and an increase in pore size diameter. Under strong basic conditions hydrophobic C_{12}–SH molecule (pore expander) can form anionic C_{12}–S^- molecules. Strong electrostatic interactions between these molecules, the cationic surfactant CTA^+ ions and the precursors will initiate a swelling process in the micelle structure [27]. Higher concentration of C_{12}–S^- molecules is expected to increase the degree of swelling and provide larger

Table 2
Physical characteristics of the synthesized mesoporous samples.

Sample code	Morphology	BET surface area (m^2/g)	Pore volume (cm^3/g)	Pore size diameter (nm)
R2	cylindrical	101.47 ± 1.5	0.972 ± 0.1	5.42 ± 0.38
R3	Spherical	78.99 ± 1.83	0.762 ± 0.24	24.48 ± 0.42
R4	foam	68.124 ± 2.12	0.66 ± 0.16	28.26 ± 0.33

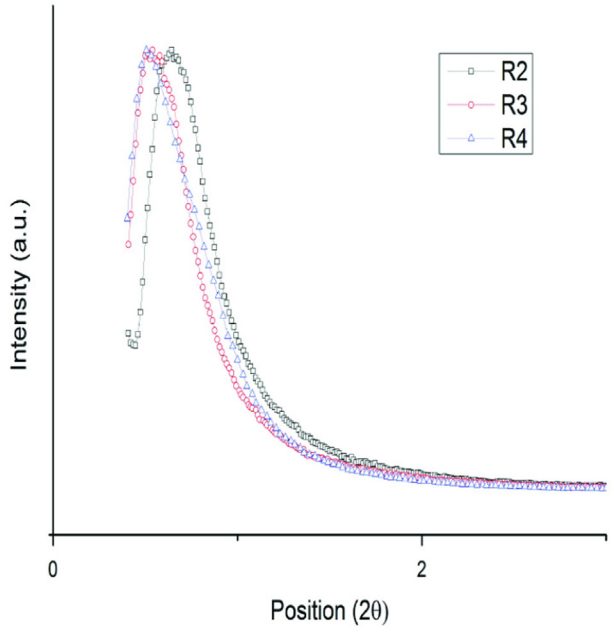

Fig. 7. Small-angle XRD patterns of synthesized mesoporous hydroxyapatite powders (R2, R3 and R4).

Table 3
Pore characteristics of the synthesized samples.

Sample code	*d* spacing (nm) *	*a* (nm) **	dp (nm) ***
R2	13.208 ± 0.36	15.53 ± 0.42	5.42 ± 0.38
R3	15.480 ± 0.59	18.21 ± 0.69	24.48 ± 0.42
R4	17.314 ± 0.35	20.36 ± 0.41	28.26 ± 0.33

*d spacing in small angle range is corresponded to the distance between crystallographic sheets.

**a corresponded to the distance between the neighboring pore centers which is determined by $\boldsymbol{a} = 2\boldsymbol{d}/\sqrt{3}$ [17] which known as unit cell parameter.

***dp, pore diameter, is calculated from the adsorption branch of the isotherm using BJH method.

pore diameter size. In the current study a fixed amount of NaOH (5 ml) was used in the synthesis of all samples. For this constant amount of NaOH solution, there should be an increase in the concentration of C_{12}–S^- molecules with the increase in the swelling agent content (samples R2–R4). The larger concentration of C_{12}–S^- molecules will provide a situation for the increase in pore diameter as indicated in Table 2. Apparently the increase in the pore size does not follow a

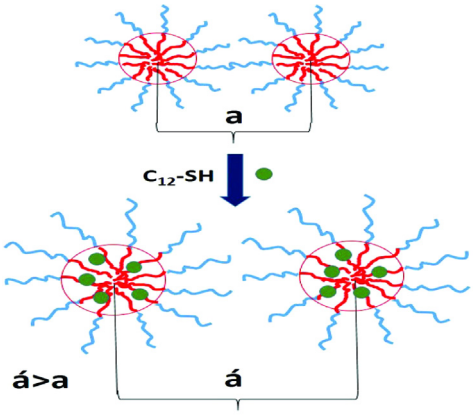

Fig. 8. Schematic presentation showing the effect of swelling agent on the distance between the pore centers (a is the distance in the absence of the swelling agent and a' is the distance in the presence of the swelling agent).

linear pattern. This may be due to the difference in the ionization degree for mediums with different NaOH/swelling agent ratios and/or some other complex interactions among the ions at higher swelling agent content. Of course there is an optimum concentration of swelling agent molecule which results in the highest pore volume and surface areas. The use of an excessive amount of this agent can lower the pore volume as indicated for the samples R3 and R4 (see Table 2). Such an observation are in agreement with the reported data in the literature [7,8]. The ordering in the pore structure was investigated by conducting small angle X-ray diffraction analysis on the samples (Fig. 7). The appearance of peaks in the range of $2\theta = 0.5$–0.7° is an indication for the presence of some degree of ordering in all samples. The calculated d spacing values, distance between the neighboring pore centers (a) and the BJH pore diameters are summarized in Table 3. As indicated in this table, the higher amount of swelling agent (higher R values) caused an increase in the pore diameter size and the distance between the pore centers which may explained by expansion of the micelle size. The role of swelling agent on the increase in the distance between the pore centers is shown schematically in Fig. 8. The shift to lower angle in small angle XRD data with the increase in the swelling agent content is the result of increased pore size and therefore the increase in the distance between the pore centers [29–31].

4. Conclusions

Mesoporous hydroxyapatite particles were synthesized by self-assembly method. It was shown that the use of swelling agent was an effective technique to control the pore characteristics in the mesoporous particles. The results showed that the use of an optimum amount of 1-dodecanethiol (swelling agent) can increase the pore diameter size and the distance between the pore centers (a). Morphological changes were observed with the increase in swelling agent content at constant surfactant concentration. A study on the effect of pore characteristics on the drug adsorption-release profiles is in progress.

References

[1] H. Oveisi, N. Suzuki, A. Beitollahi, Y. Yamauchi, J. Sol–Gel Sci. Technol. 56 (2) (2010) 212–218.
[2] H. Oveisi, A. Beitollahi, M. Imura, C.W. Wu, Y. Yamauchi, Microporous Mesoporous Mater. 134 (1–3) (2010) 150–156.
[3] P.J. Pannone, Trends in biomaterials research, Nova Science Pub Incorporated, New York, 2007, p. 115.
[4] Y. Dou, S. Cai, X. Ye, G. Xu, H. Hu, X. Ye, J. Sol–Gel Sci. Technol. 61 (1) (2011) 126–132.
[5] Y. Deng, Y. Cai, Z. Sun, D. Zhao, Chem. Phys. Lett. 510 (1) (2011) 1–13.
[6] M. Vallet Regí, F. Balas, D. Arcos, Angew. Chem. Int. Ed. 46 (40) (2007) 7548–7558.
[7] Y.K. Hwang, K.R. Patil, S.H. Jhung, J.S. Chang, Y.J. Ko, S.E. Park, Microporous Mesoporous Mater. 78 (2–3) (2005) 245–253.
[8] A.S. Poyraz, J. phys. chem. C 113 (2009) 18596–18607.
[9] M. Sadat-Shojai, M.-T. Khorasani, E. Dinpanah-Khoshdargi, A. Jamshidi, Acta Biomater. 9 (8) (2013) 7591–7621.
[10] H. Fu, M.N. Rahaman, R.F. Brown, D.E. Day, Mater. Sci. Eng. C 33 (4) (2011) 2245–2250.
[11] H. Fu, M.N. Rahaman, D.E. Day, R.F. Brown, J. Mater. Sci. Mater. Med. 22 (3) (2011) 579–591.
[12] W. Xiao, H. Fu, M.N. Rahaman, Y. Liu, B. Sonny Bal, Acta Biomater. 9 (9) (2013) 8374–8383.
[13] J. Yao, W. Tjandra, Y.Z. Chen, K.C. Tam, J. Ma, B. Soh, J. Mater. Chem. 13 (12) (2003) 3053–3057.
[14] Y. Wu, S. Bose, Langmuir 21 (8) (2005) 3232–3234.
[15] F. Ye, H. Guo, H. Zhang, X. He, Acta Biomater. 6 (6) (2010) 2212–2218.
[16] Y. Jiao, Y.P. Lu, G.Y. Xiao, W.H. Xu, R.F. Zhu, Powder Technol. 217 (2012) 581–584.
[17] Y. Li, W. Tjandra, K.C. Tam, Mater. Res. Bull. 43 (8–9) (2008) 2318–2326.
[18] P.M.S.L. Shanthi, R.V. Mangalaraja, A.P. Uthirakumar, S. Velmathi, T. Balasubramanian, M. Ashok, J. Colloid Interface Sci. 350 (1) (2010) 39–43.
[19] D. Gopi, J. Indira, L. Kavitha, M. Sekar, U.K. Mudali, Spectrochim. Acta A. Mol. Biomol. Spectrosc. 93 (2012) 131–134.
[20] S.K. Saha, A. Banerjee, S. Banerjee, S. Bose, Mater. Sci. Eng. C 29 (7) (2009) 2294–2301.
[21] E. Salimi, J. Javadpour, M. Anbia, Template-Based Synthesis of Nanoporous Hydroxyapatite, ISRN Ceram. 2012 (2012) 1–6.
[22] Q. Zhao, T. Wang, J. Wang, L. Zheng, T. Jiang, G. Cheng, S. Wang J. Non-Cryst. Solids 358 (2) (2012) 229–235.
[23] M. Sadat-Shojai, M.T. Khorasani, A. Jamshidi, J. Cryst. Growth 361 (2012) 73–84.
[24] N. Pramanik, T. Imae, Langmuir 28 (39) (2012) 14018–14027.
[25] G. Verma, K.C. Barick, N. Manoj, A.K. Sahu, P.A. Hassan, Ceram. Int. 39 (8) (2013) 8995–9002.
[26] J.S. Lettow, Y.J. Han, P. Schmidt-Winkel, P. Yang, D. Zhao, G. D. Stucky, J.Y. Ying, Langmuir 16 (22) (2000) 8291–8295.
[27] H. Chen, T. Hu, X. Zhang, K. Huo, P.K. Chu, J. He, Langmuir 26 (16) (2010) 13556–13563.
[28] Y.S. Lee, Self-assembly and nanotechnology: a force balance approach, John Wiley & Sons, United States of America, 2008, p. 68.
[29] C. Jiang, K. Zhou, X. Zhong, H. Zhong, Powder Technol. 259 (2014) 74–80.
[30] Y. Deng, J. Liu, C. Liu, D. Gu, Z. Sun, J. Wei, J. Zhang, L. Zhang, B. Tu, D. Zhao, Chem. Mater. 20 (23) (2008) 7281–7286.
[31] J. Feng, B. Sun, Y. Yao, S. Che, Microporous Mesoporous Mater. 172 (2013) 30–35.